nature ecology & evolution

Article

https://doi.org/10.1038/s41559-023-02091-z

Low morphological disparity and decelerated rate of limb size evolution close to the origin of birds

In the format provided by the authors and unedited

CONTENTS:

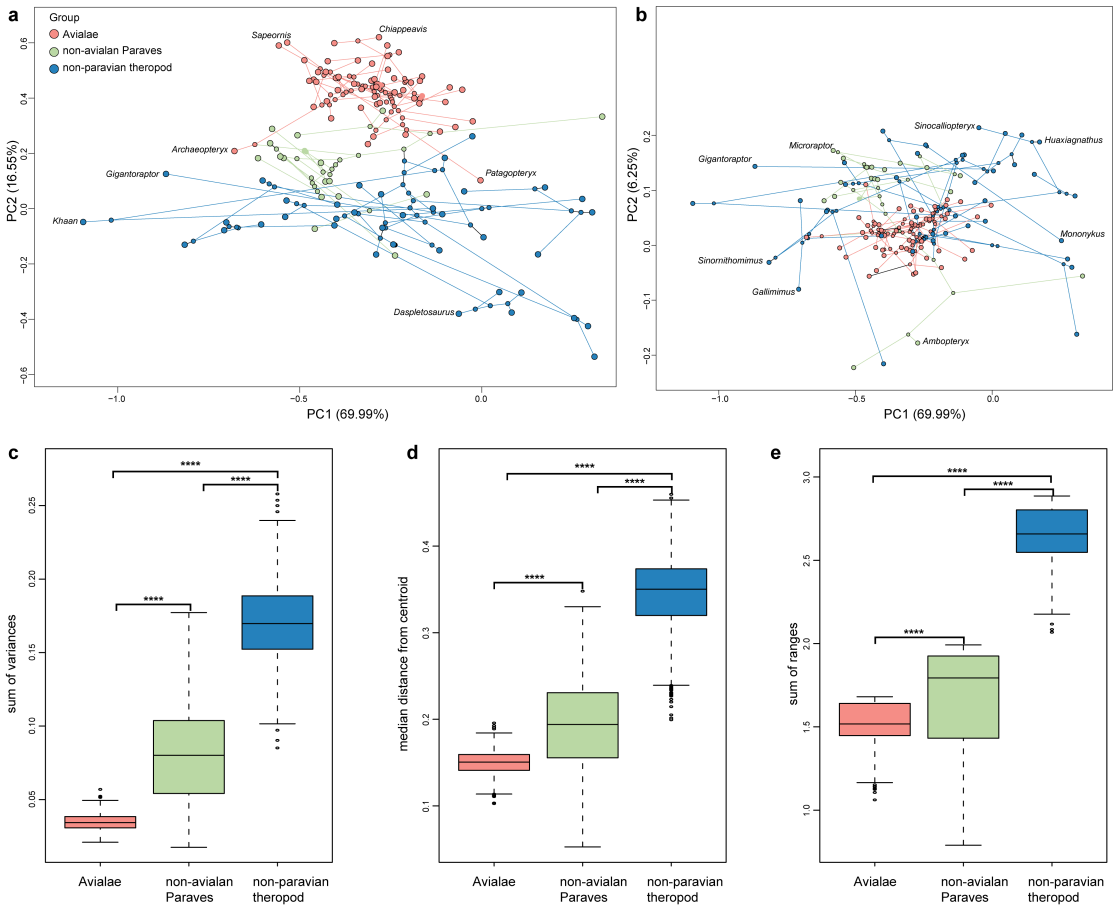

Supplementary Fig. 1. Morphological disparity of appendicular elements of Mesozoic theropods. The result is derived from super tree II. **a, b,** Phylomorphospace of the first three principal components (PCs) of both fore- and hindlimb elements. **c–e**, Comparison of morphological disparity among subgroups of Mesozoic theropods (The boxes represent the median, the first and the third quartile of the disparity; n = 109 species): sum of variances (**c**), median distance from centroid (**d**), and sum of ranges (**e**). Morphological disparity was compared using Welch's t-test for statistical significance (****two-sided p-value threshold <0.05).

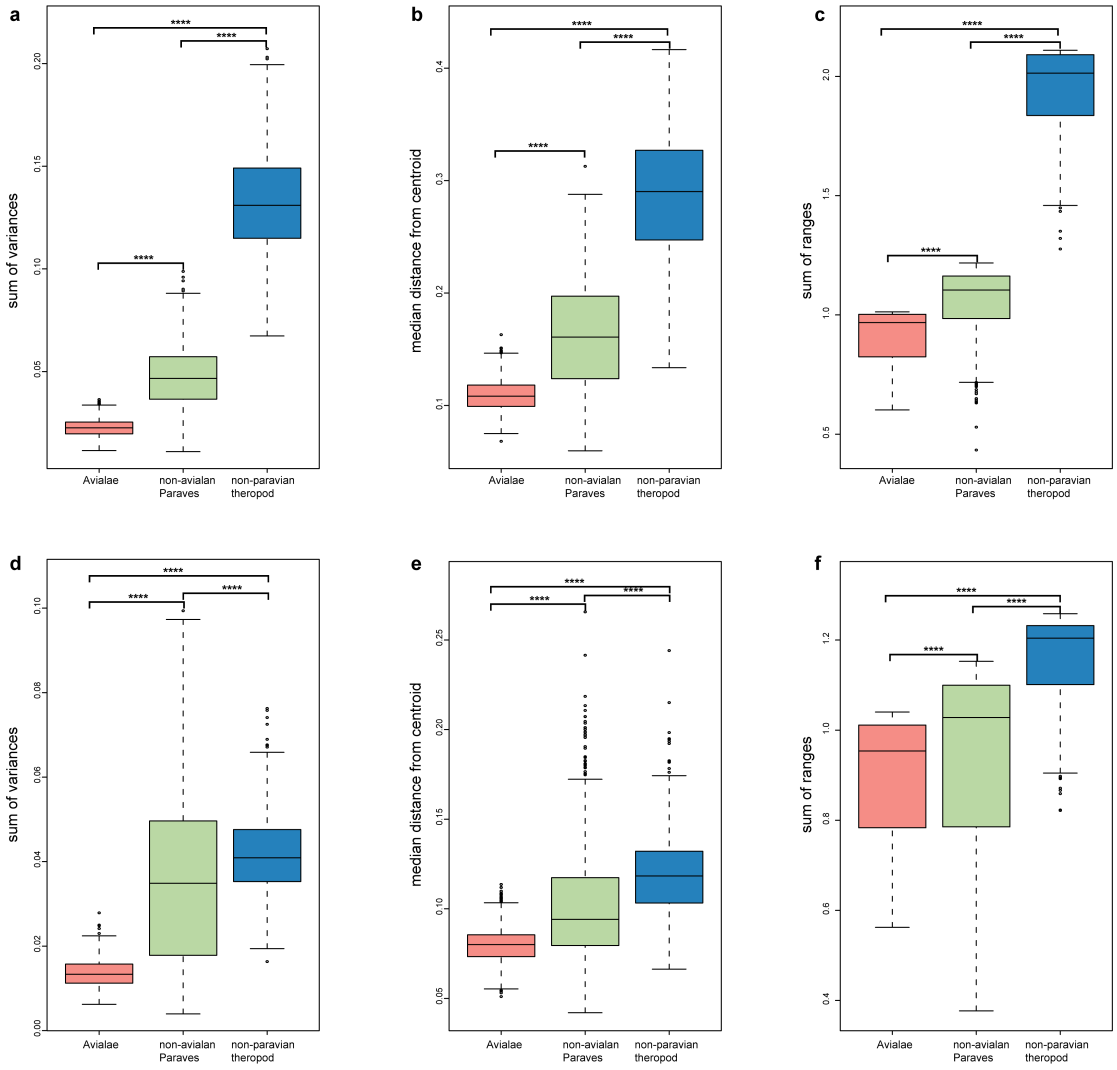

Supplementary Fig. 2. Comparison of morphological disparity of forelimb and hindlimb among Mesozoic theropods. The result is derived from super tree II. **a–c**, Forelimb. **d–e,** Hindlimb. Morphological disparity is quantified using three metrics: sum of variances (**a, d**), median distance from centroid (**b, e**), and sum of ranges (**c, f**). The boxes represent the median, the first and the third quartile of the disparity; *n* = 109 species (**a–f**). Morphological disparity was compared using Welch's *t*-test for statistical significance (****two-sided *p*-value threshold <0.05).

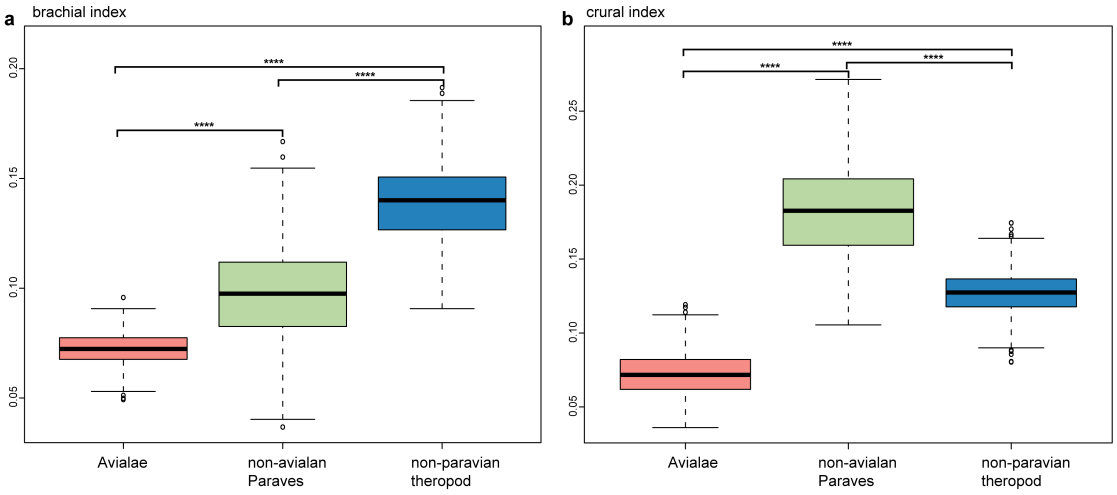

Supplementary Fig. 3. Comparison of two functional indices of Mesozoic theropods. The result is derived from super tree II. **a,** Branchial index (*n* = 109 species). **b,** Crural index (*n* = 109 species). The boxes represent the median, the first and the third quartile of the disparity. Morphological disparity was compared using Welch's *t*-test for statistical significance (****two-sided *p*-value threshold <0.05).

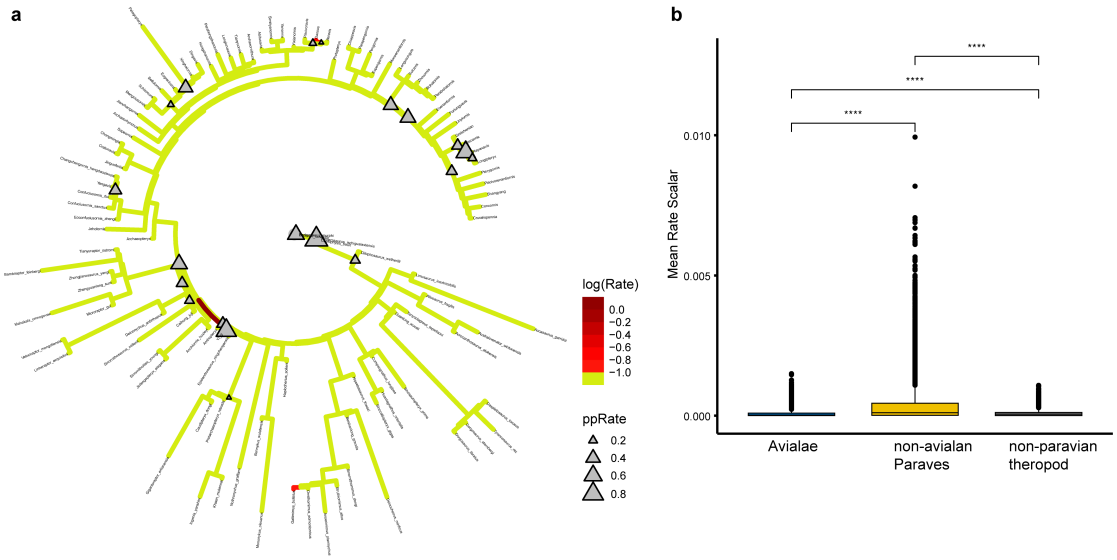

Supplementary Fig. 4. Evolutionary rate and rate shift of appendicular elements of Mesozoic theropods. The result is derived from super tree II. **a,** Branch specific evolutionary rates and rate shifts of all limb elements (Branch specific evolutionary rates are denoted by the color gradients. Posterior probabilities of rate shifts are indicated by the relative size of the grey triangles). **b,** Comparison of evolutionary rate of subgroups of Mesozoic theropods (The boxes represent the median, the first and the third quartile of the mean rate scalar; n = 109 species). The mean rate scalar is the mean of the rate scalars calculated in the post-burn-in posterior distribution under the variable rate evolutionary model. Evolutionary rate among subgroups were compared using a nonparametric t-test for statistical significance (****: $p < 0.00005$).

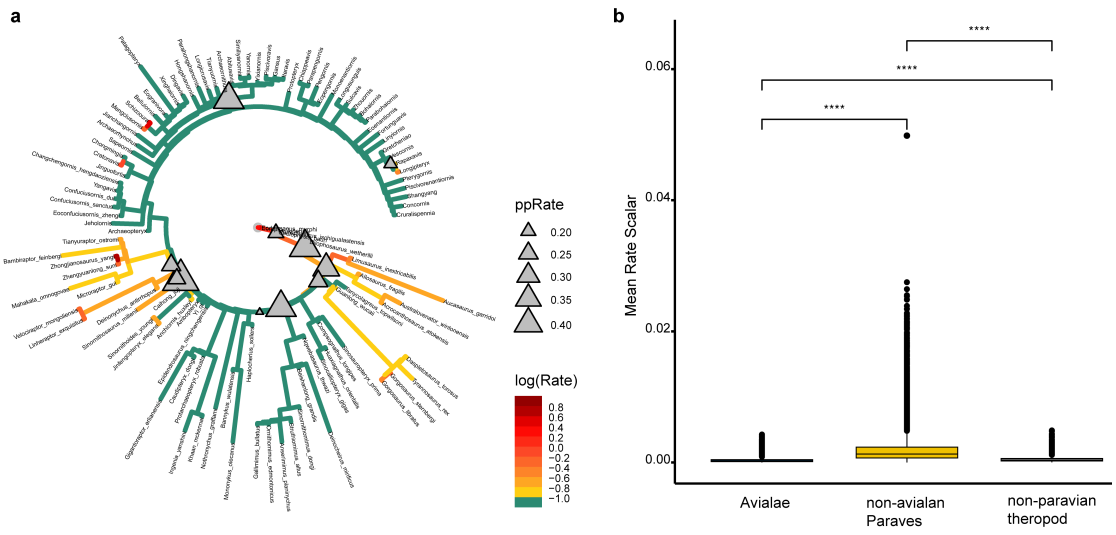

Supplementary Fig. 5. Evolutionary rate and rate shift of brachial index across Mesozoic theropod phylogeny. The result is derived from super tree II. **a,** Branch specific evolutionary rates and rate shifts (Branch specific evolutionary rates are denoted by the color gradients. Posterior probabilities of rate shifts are indicated by the relative size of the grey triangles). **b,** Comparison of evolutionary rate of subgroups of Mesozoic theropods (The boxes represent the median, the first and the third quartile of the mean rate scalar; n = 109 species). The mean rate scalar is the mean of the rate scalars calculated in the post-burn-in posterior distribution under the variable rate evolutionary model. Evolutionary rate among subgroups were compared using a nonparametric t-test for statistical significance (****: $p < 0.00005$).

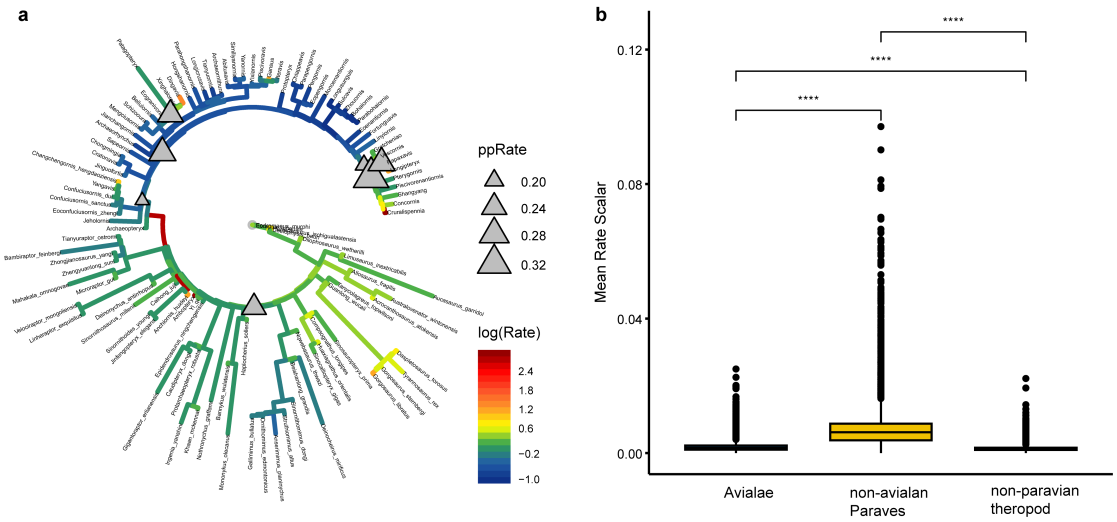

Supplementary Fig. 6. Evolutionary rate and rate shift of crural index across Mesozoic theropod phylogeny. The result is derived from super tree II. **a,** Branch specific evolutionary rates and rate shifts (Branch specific evolutionary rates are denoted by the color gradients. Posterior probabilities of rate shifts are indicated by the relative size of the grey triangles). **b,** Comparison of evolutionary rate of subgroups of Mesozoic theropods (The boxes represent the median, the first and the third quartile of the mean rate scalar; n = 109 species). The mean rate scalar is the mean of the rate scalars calculated in the post-burn-in posterior distribution under the variable rate evolutionary model. Evolutionary rate among subgroups were compared using a nonparametric t-test for statistical significance (****: $p < 0.00005$).

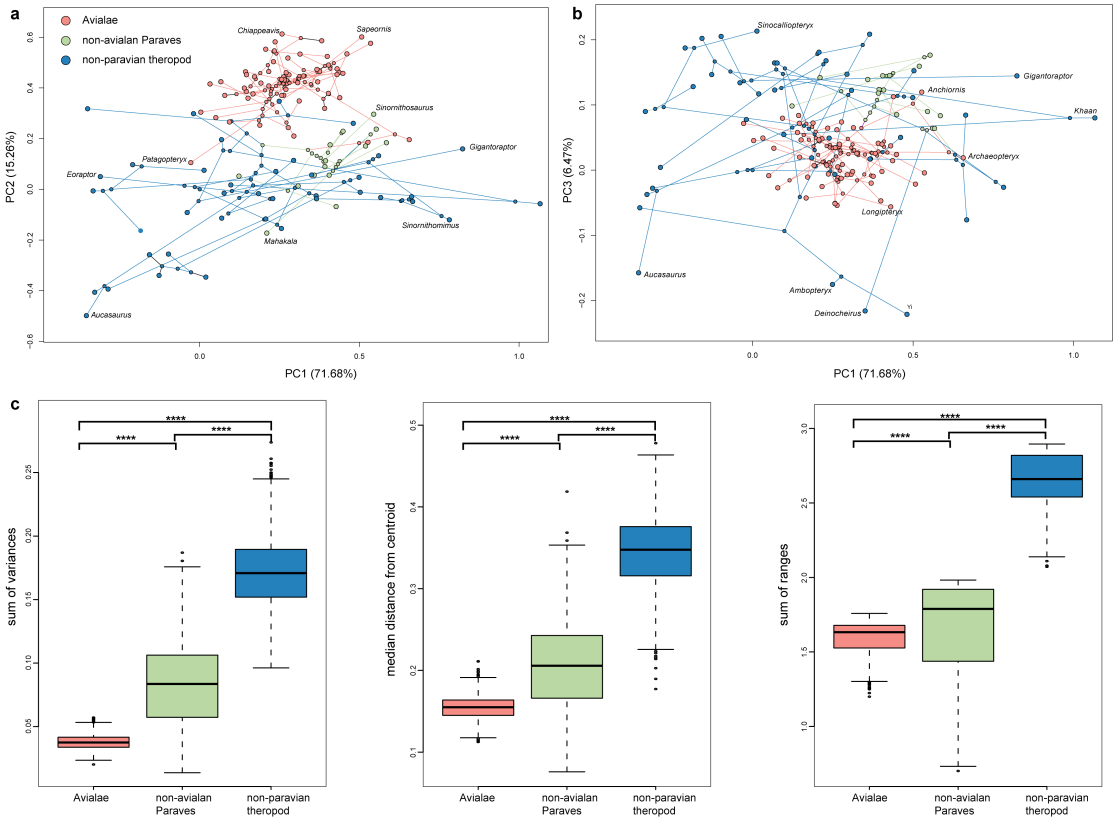

Supplementary Fig. 7. Morphological disparity of appendicular elements of Mesozoic theropods. The result is derived from super tree III. **a, b,** Phylomorphospace of the first three principal components (PCs) of both fore- and hindlimb elements. **c**, Comparison of morphological disparity among subgroups of Mesozoic theropods (The boxes represent the median, the first and the third quartile of the morphological disparity; n = 109 species). Morphological disparity was compared using Welch's t-test for statistical significance (****two-sided p-value threshold <0.05).

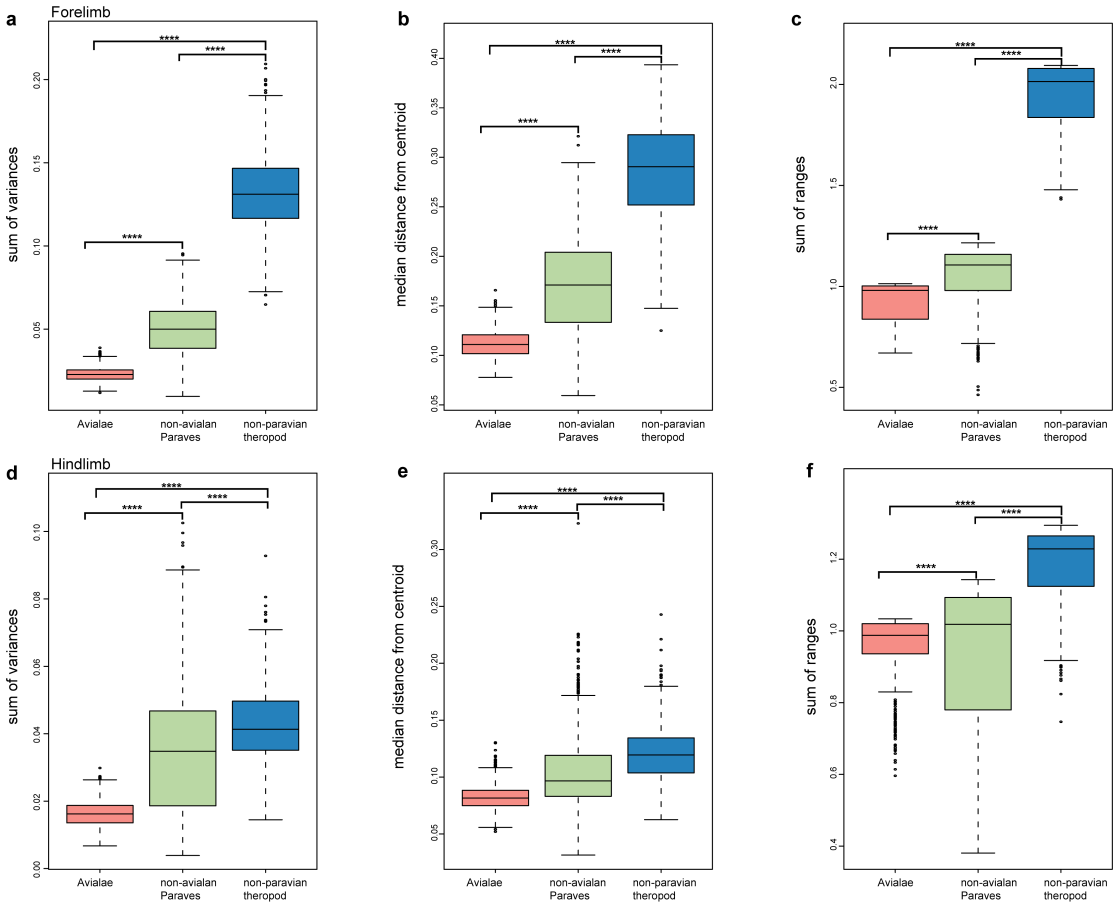

Supplementary Fig. 8. Comparison of morphological disparity of forelimb and hindlimb among Mesozoic theropods. The result is derived from super tree III. **a–c**, Forelimb. **d–e,** Hindlimb. Morphological disparity is quantified using three metrics (The boxes represent the median, the first and the third quartile of the morphological disparity; n = 109 species): sum of variances (**a, d**), median distance from centroid (**b, e**), and sum of ranges (**c, f**). Morphological disparity was compared using Welch's *t*-test for statistical significance (****two-sided *p*-value threshold <0.05).

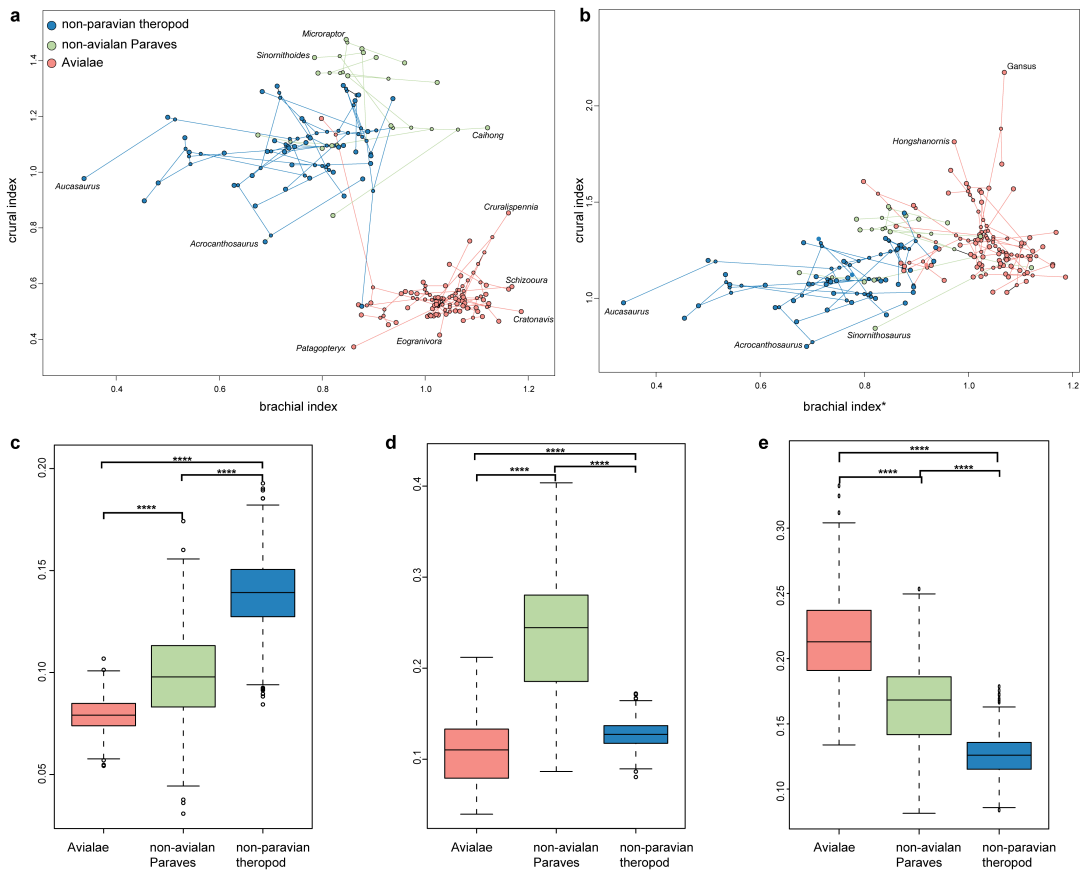

Supplementary Fig. 9. Evolutionary changes of brachial (BI) and crural (CI) indices across Mesozoic theropod phylogeny. The result is derived from super tree III. **a,** Phylomorphospace of BI and crural CI (CI is calculated differently for avialan and non-avialan taxa; see Method); **b,** Phylomorphospace of BI and crural CI (CI is calculated the same way for avialan and non-avialan taxa; see Method). **c–e,** Comparison of disparity among three subgroups using standard deviations of BI (**c**) and CI (**d:** CI is calculated differently for avialan and non-avialan taxa; **e:** CI is calculated the same way for avialan and non-avialan taxa. The boxes represent the median, the first and the third quartile of the morphological disparity (n = 109 species). Morphological disparity was compared using Welch's t-test for statistical significance (****two-sided p-value threshold <0.05).

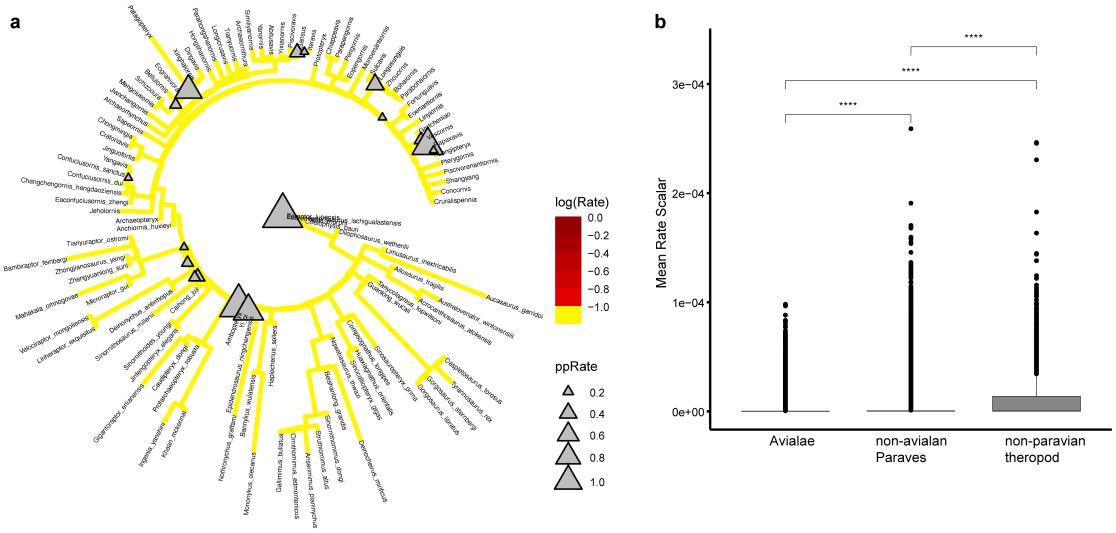

Supplementary Fig. 10. Evolutionary rate and rate shift of appendicular elements of Mesozoic theropods. The result is derived from super tree III. **a,** Branch specific evolutionary rates and rate shifts of all limb elements (Branch specific evolutionary rates are denoted by the color gradients. Posterior probabilities of rate shifts are indicated by the relative size of the grey triangles). **b,** Comparison of evolutionary rate of subgroups of Mesozoic theropods (The boxes represent the median, the first and the third quartile of the mean rate scalar; n = 109 species). The mean rate scalar is the mean of the rate scalars calculated in the post-burn-in posterior distribution under the variable rate evolutionary model. Evolutionary rate among subgroups were compared using a nonparametric t-test for statistical significance (****: $p < 0.00005$).

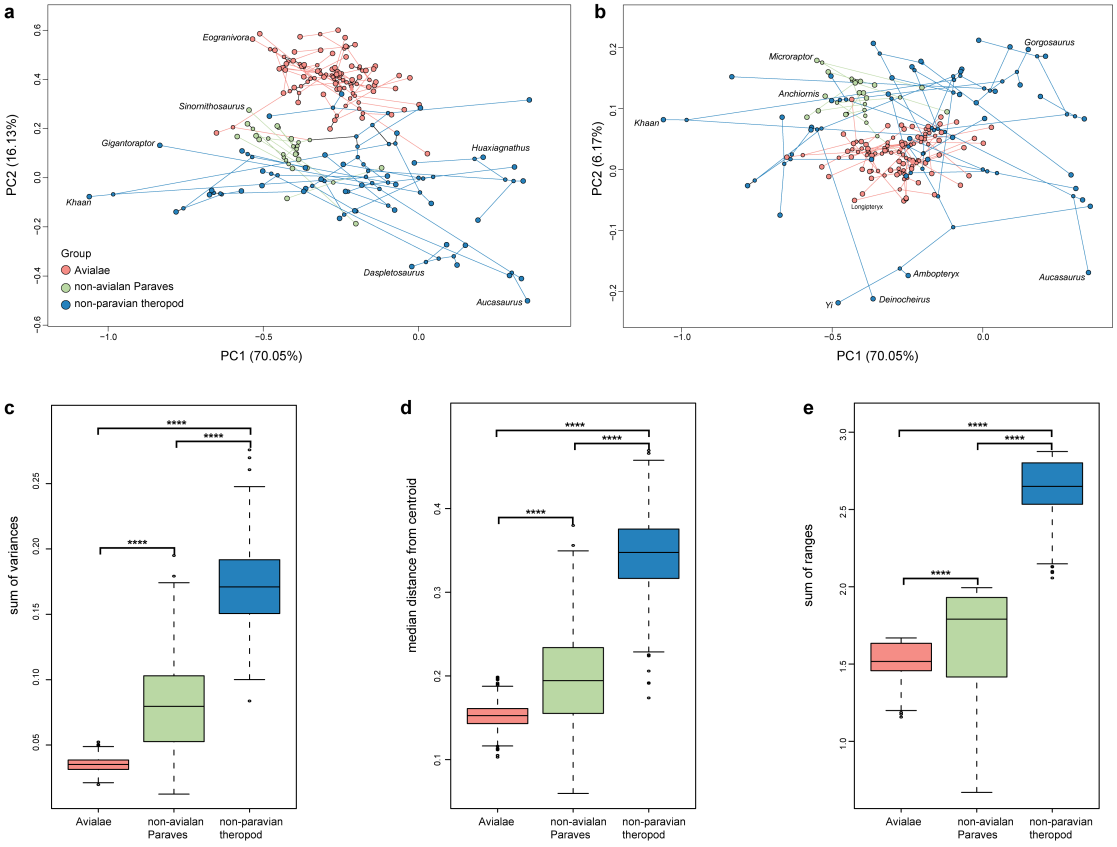

Supplementary Fig. 11. Morphological disparity of appendicular elements of Mesozoic theropods. The result is derived from super tree IV. **a, b,** Phylomorphospace of the first three principal components (PCs) of both fore- and hindlimb elements. **c–e**, Comparison of morphological disparity among subgroups of Mesozoic theropods (The boxes represent the median, the first and the third quartile of the morphological disparity; n = 109 species): sum of variances (**c**), median distance from centroid (**d**), and sum of ranges (**e**). Morphological disparity was compared using Welch's t-test for statistical significance (****two-sided p-value threshold <0.05).

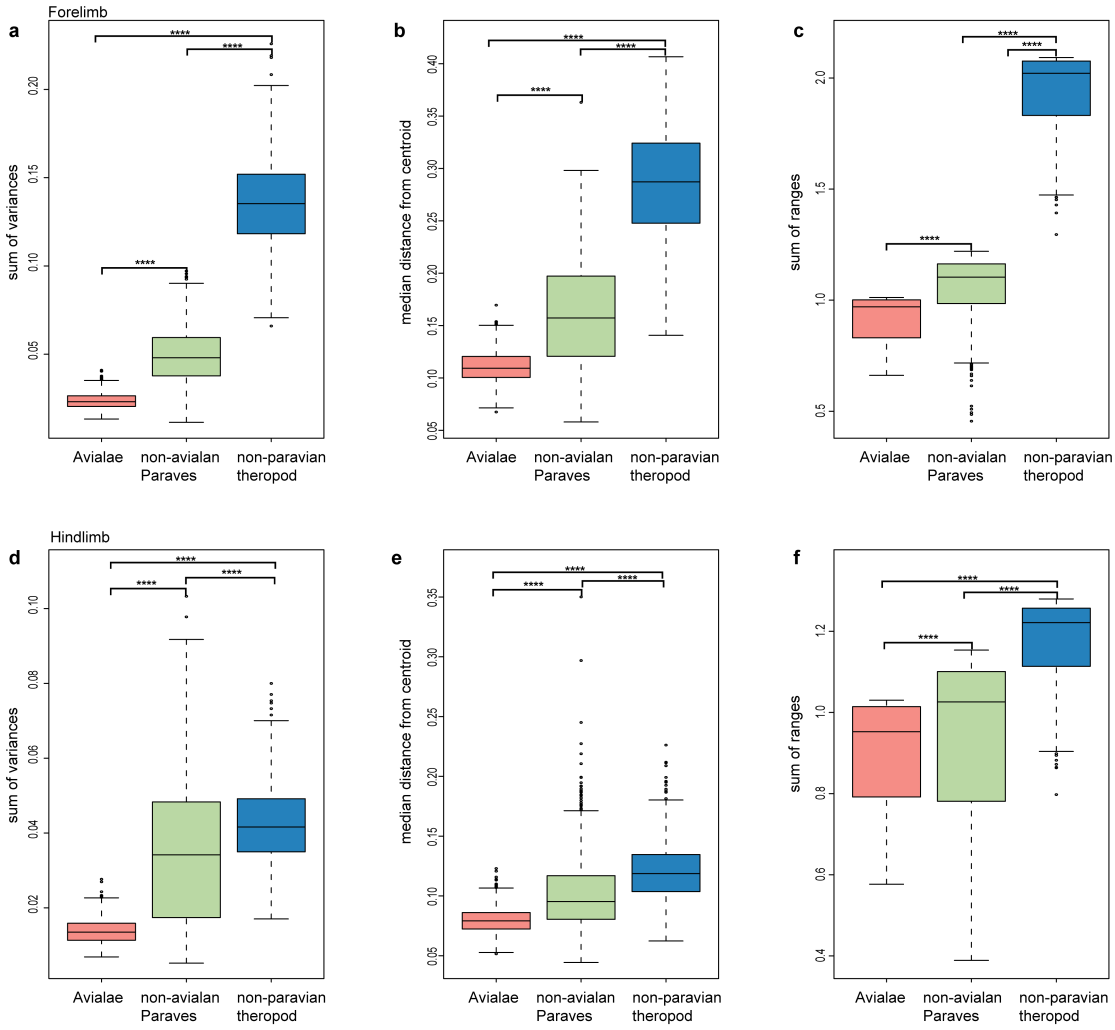

Supplementary Fig. 12. Comparison of morphological disparity of forelimb and hindlimb among Mesozoic theropods. The result is derived from super tree IV. **a–c**, Forelimb. **d–e,** Hindlimb. Morphological disparity is quantified using three metrics: sum of variances (**a, d**), median distance from centroid (**b, e**), and sum of ranges (**c, f**). The boxes represent the median, the first and the third quartile of the morphological disparity; n = 109 species (**a–f**). Morphological disparity was compared using Welch's t-test for statistical significance (****two-sided p-value threshold <0.05).

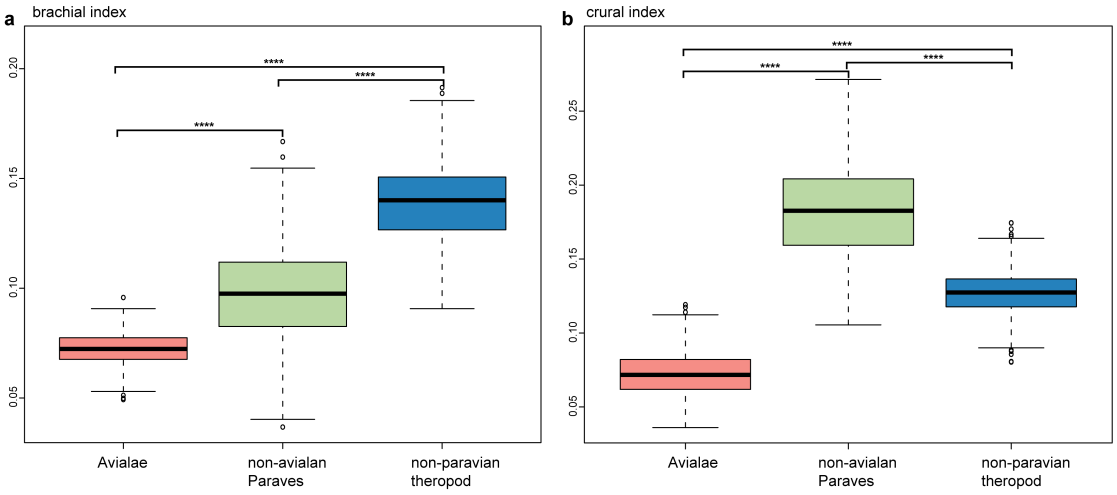

Supplementary Fig. 13. Comparison of two functional indices of Mesozoic theropods. The result is derived from super tree IV. **a,** Branchial index. **c,** Crural index (CI is calculated differently for avialan and non-avialan taxa; see Method). The boxes represent the median, the first and the third quartile of the morphological disparity; n = 109 species (**a,b**) Morphological disparity was compared using Welch's t-test for statistical significance (****two-sided p-value threshold <0.05).

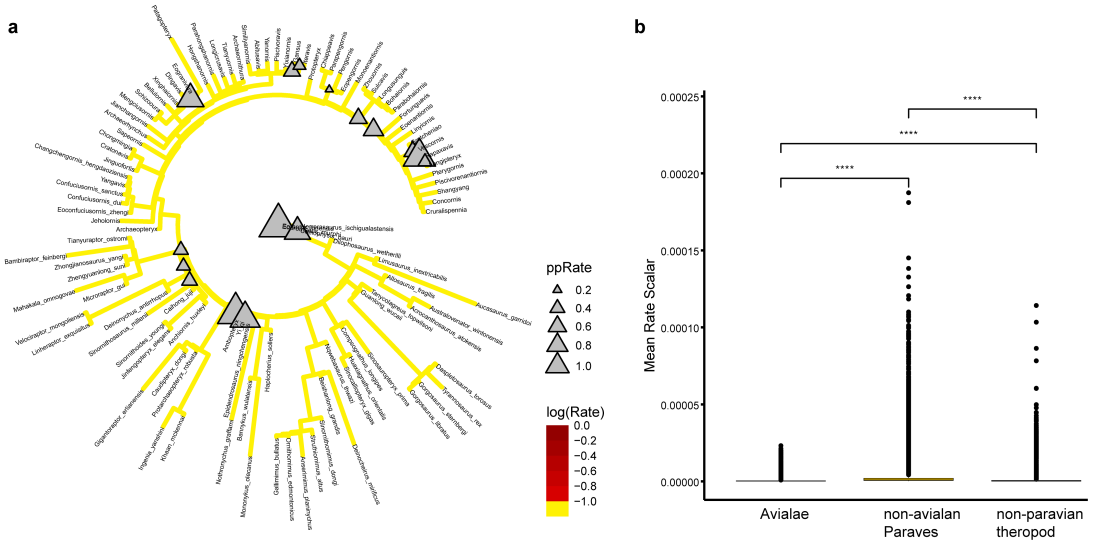

Supplementary Fig. 14. Evolutionary rate and rate shift of appendicular elements of Mesozoic theropods. The result is derived from super tree IV. **a,** Branch specific evolutionary rates and rate shifts of all limb elements (Branch specific evolutionary rates are denoted by the color gradients. Posterior probabilities of rate shifts are indicated by the relative size of the grey triangles). **b,** Comparison of evolutionary rate of subgroups of Mesozoic theropods (The boxes represent the median, the first and the third quartile of the mean rate scalar; n = 109 species). The mean rate scalar is the mean of the rate scalars calculated in the post-burn-in posterior distribution under the variable rate evolutionary model. Evolutionary rate among subgroups were compared using a nonparametric t-test for statistical significance (****: $p < 0.00005$).

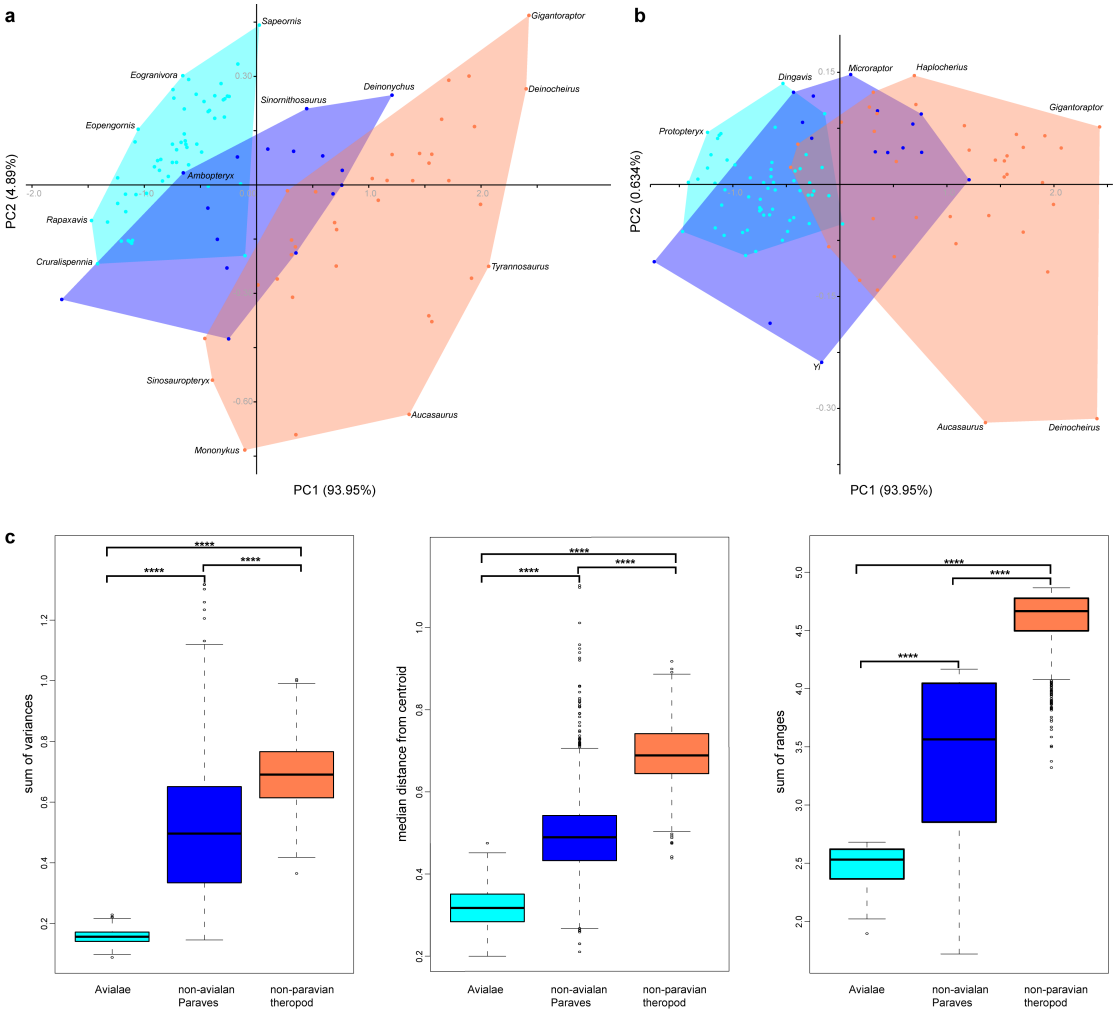

Supplementary Fig. 15. Morphological disparity of appendicular elements of Mesozoic theropods. The result is derived from super tree I. **a, b,** Morphospace of the first three principal components (PCs) of both fore- and hindlimb elements derived from conventional PCA. **c**, Comparison of morphological disparity among subgroups of Mesozoic theropods (The boxes represent the median, the first and the third quartile of the morphological disparity; n = 109 species). Morphological disparity was compared using Welch's t-test for statistical significance (****two-sided p-value threshold <0.05).

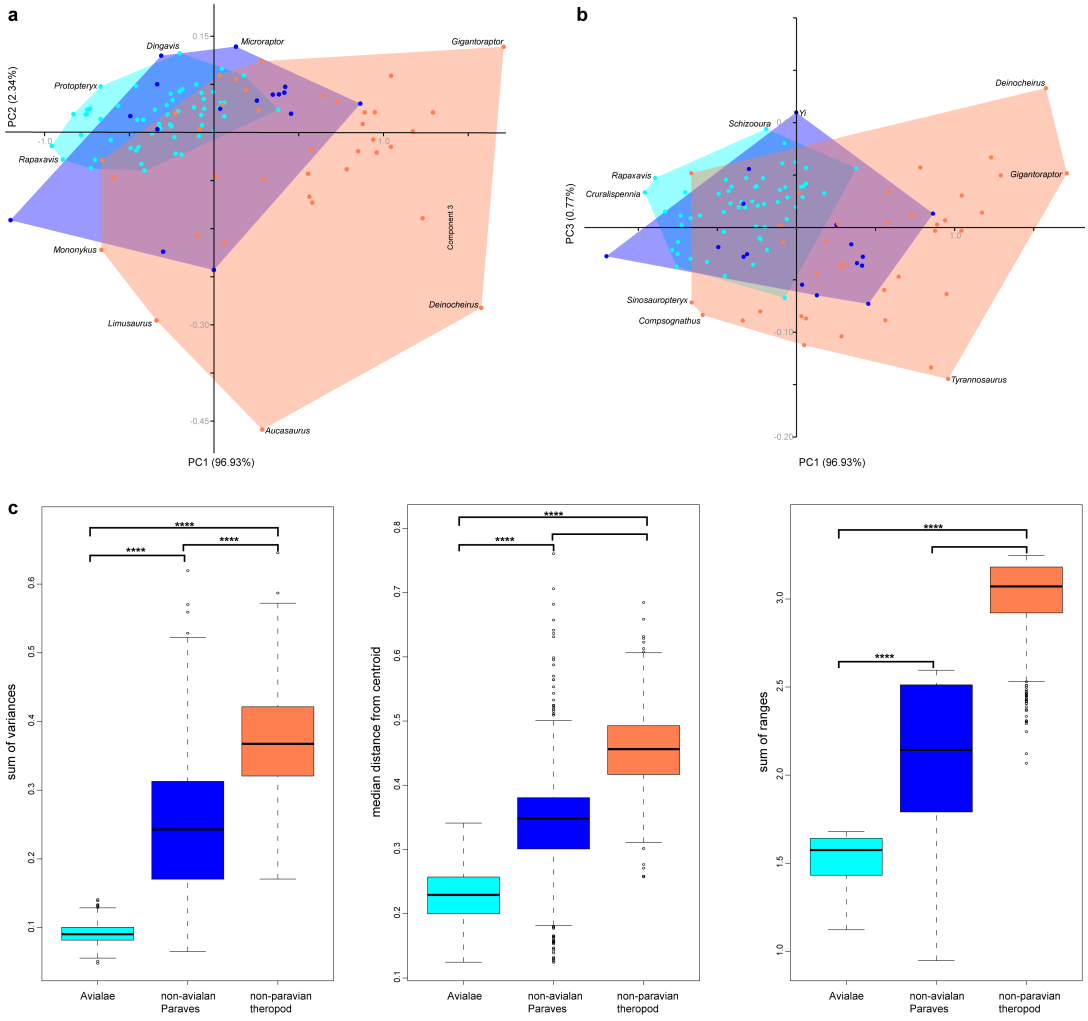

Supplementary Fig. 16. Morphological disparity of forelimb of Mesozoic theropods. The result is derived from super tree I. **a, b,** Morphospace of the first three principal components (PCs) of forelimb elements derived from conventional PCA. **c**, Comparison of morphological disparity among subgroups of Mesozoic theropods (The boxes represent the median, the first and the third quartile of the morphological disparity; n = 109 species). Morphological disparity was compared using Welch's t-test for statistical significance (****two-sided p-value threshold <0.05).

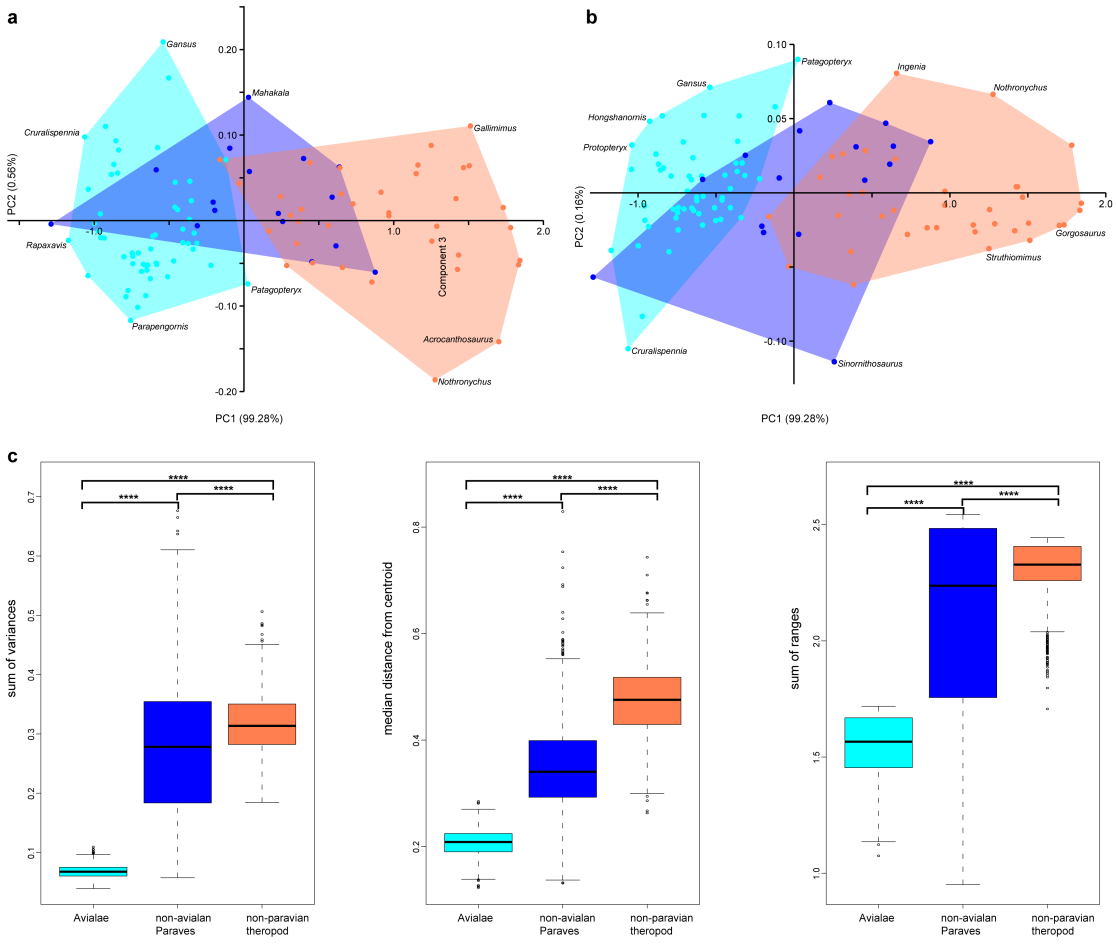

Supplementary Fig. 18. Morphological disparity of hindlimb of Mesozoic theropods. The result is derived from super tree I. **a, b,** Morphospace of the first three principal components (PCs) of hindlimb elements derived from conventional PCA. **c**, Comparison of morphological disparity among subgroups of Mesozoic theropods (The boxes represent the median, the first and the third quartile of the morphological disparity; n = 109 species). Morphological disparity was compared using Welch's t-test for statistical significance (****two-sided p-value threshold <0.05).

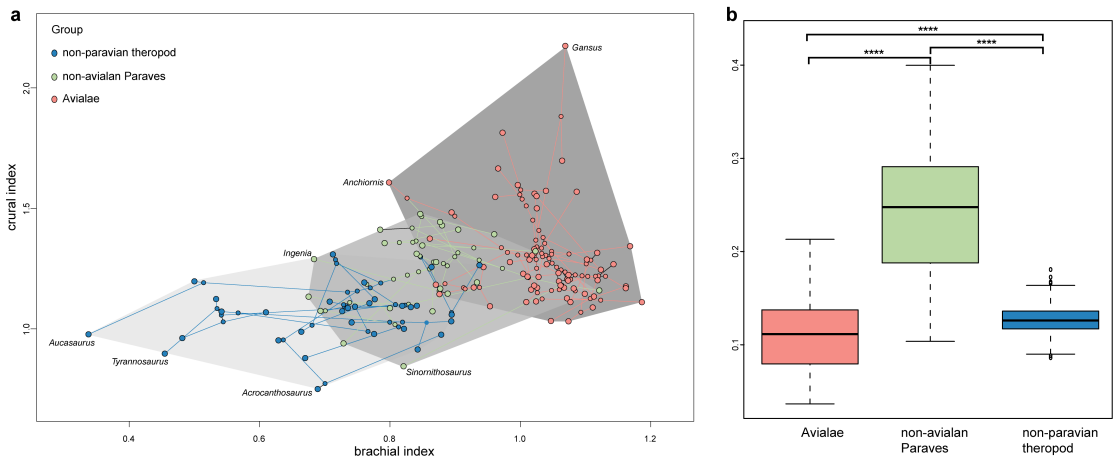

Supplementary Fig. 18. Evolutionary changes of brachial (BI) and crural (CI) indices across Mesozoic theropod phylogeny. The result is derived from super tree I. **a,** Phylomorphospace of BI and crural CI (CI is calculated the same way for avialan and non-avialan taxa; see Method); **b,** Comparison of disparity among three subgroups using standard deviations (The boxes represent the median, the first and the third quartile of the morphological disparity; n = 109 species). Morphological disparity was compared using Welch's t-test for statistical significance (****two-sided p-value threshold <0.05).

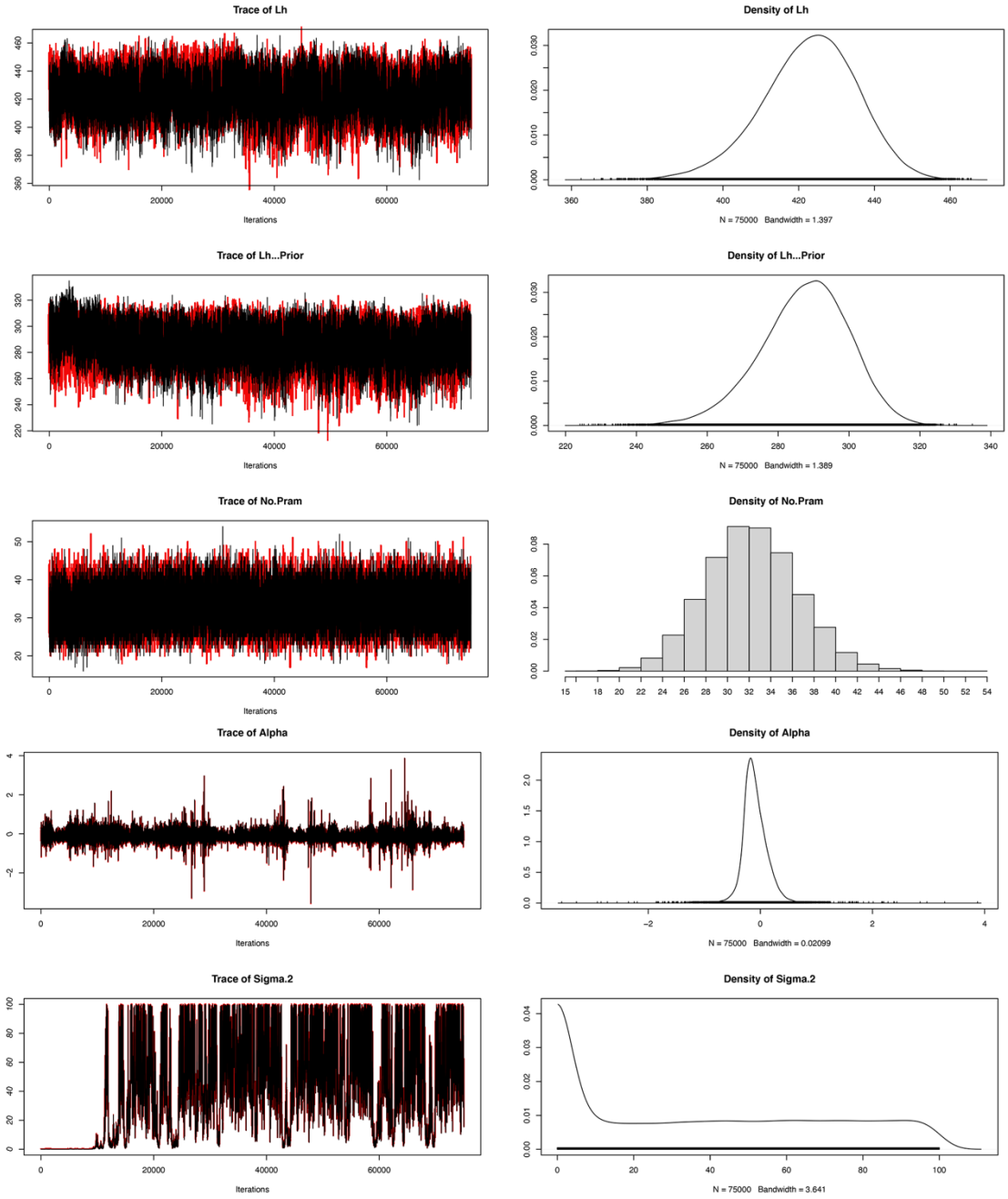

Supplementary Fig. 19. Results of trace plot and Gelman and Rubin's convergence diagnostic for checking parameter and model convergence for two independent rjMCMC analyses of all limb measurements.

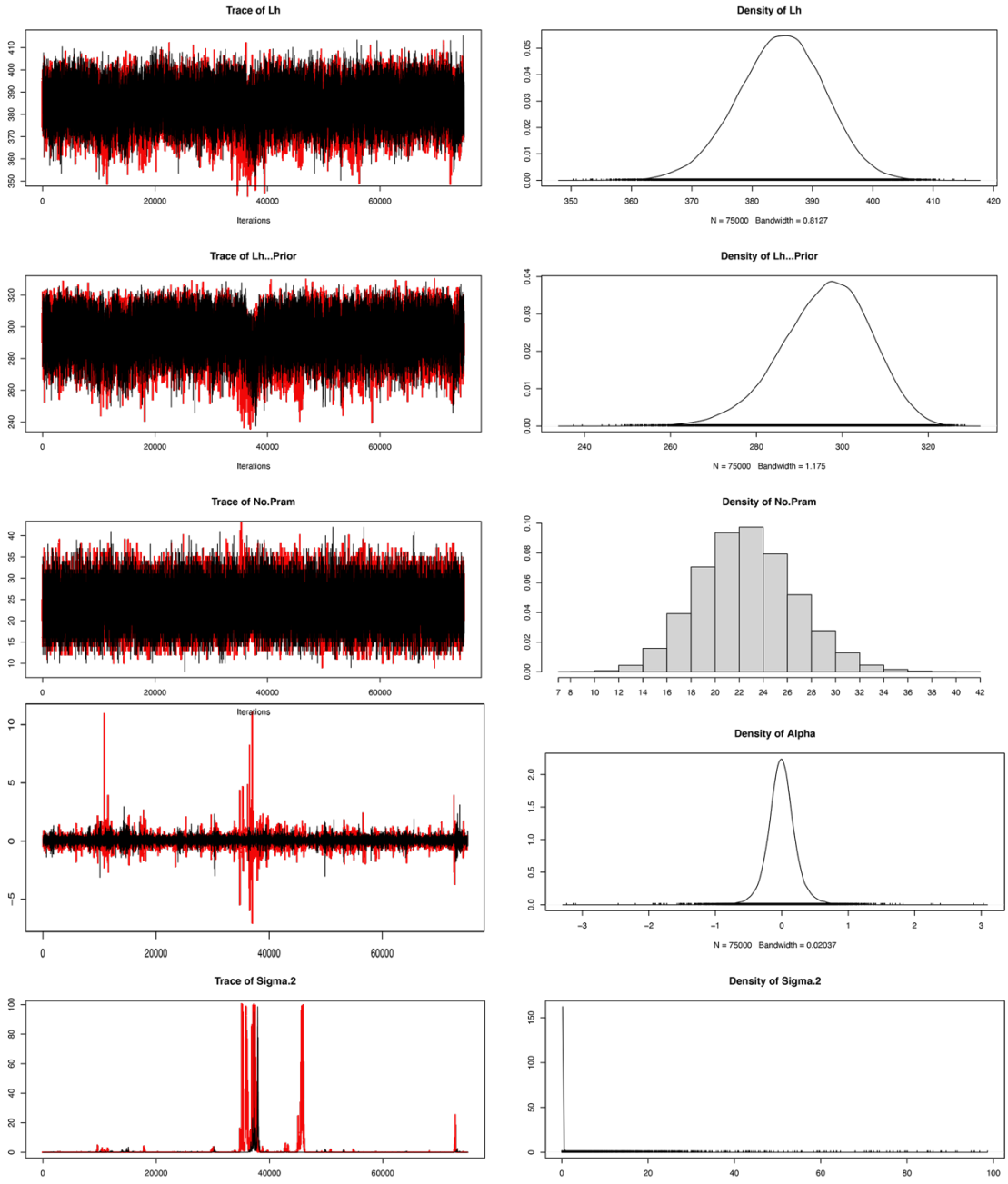

Supplementary Fig. 20. Results of trace plot and Gelman and Rubin's convergence diagnostic for checking parameter and model convergence for two independent rjMCMC analyses of forelimb measurements.

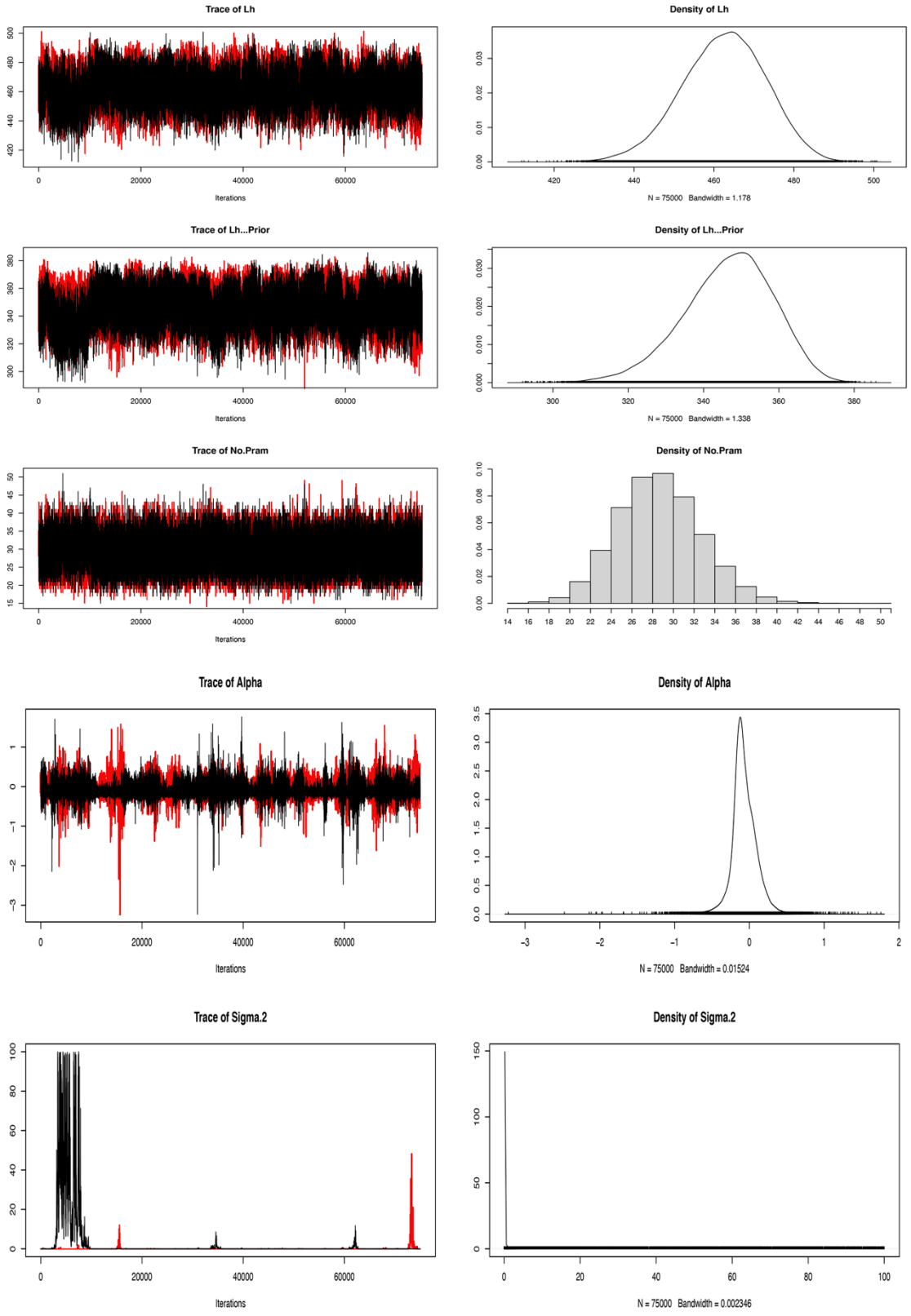

Supplementary Fig. 21. Results of trace plot and Gelman and Rubin's convergence diagnostic for checking parameter and model convergence for two independent rjMCMC analyses of hindlimb measurements.

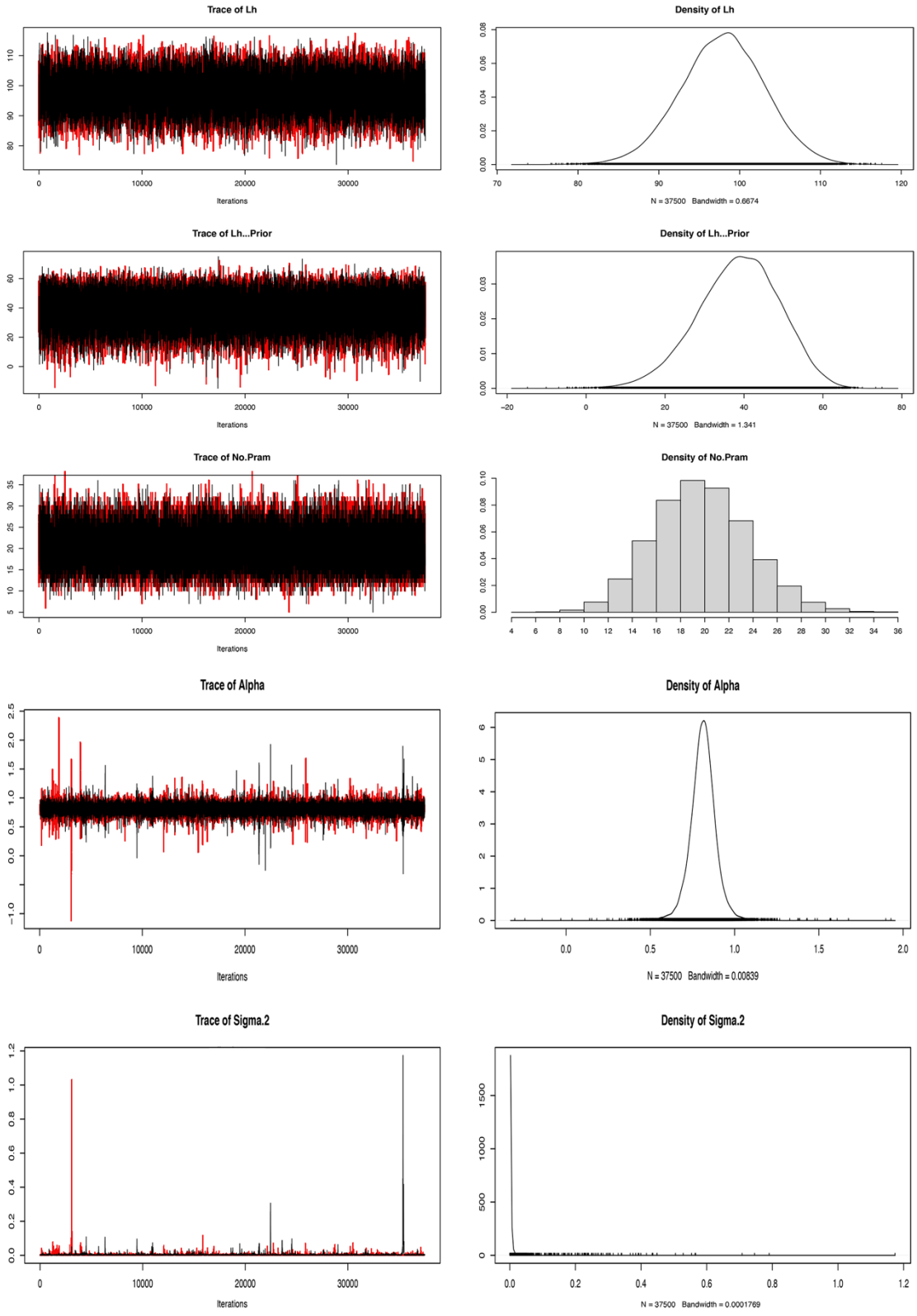

Supplementary Fig. 22. Results of trace plot and Gelman and Rubin's convergence diagnostic for checking parameter and model convergence for two independent rjMCMC analyses of brachial index.

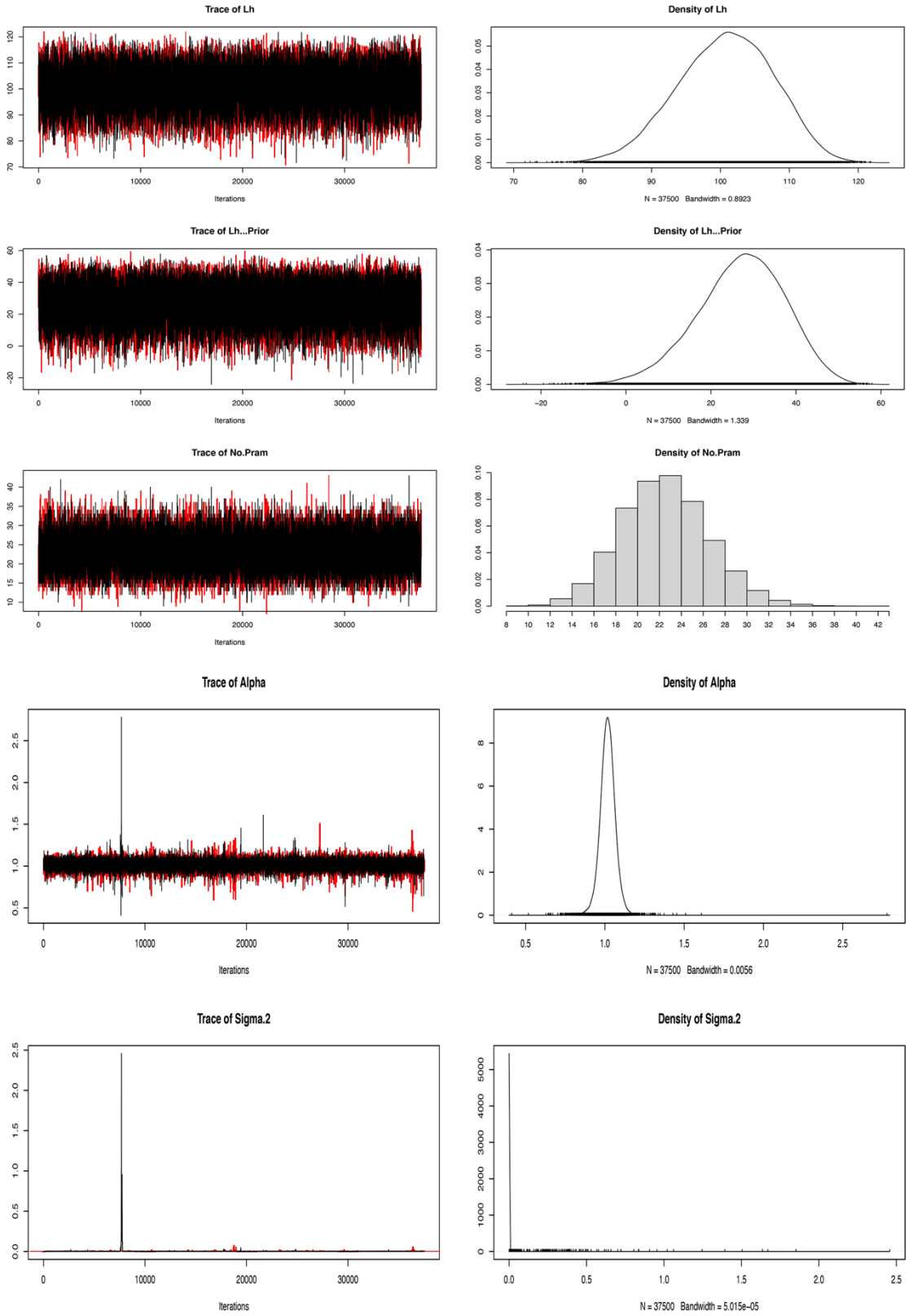

Supplementary Fig. 23. Results of trace plot and Gelman and Rubin's convergence diagnostic for checking parameter and model convergence for two independent rjMCMC analyses of crural index.

Supplementary Table 1. List of taxonomical sampling (in separated Excel file)

Supplementary Table 2. Results of phylogenetically principal components analysis using the all limb elements of Mesozoic theropods. The phylogeny backbone derived from the "mbl"-scaled super tree I.

	PC1	PC2	PC3	PC4	PC5	PC6
Standard deviation	0.0821	0.0398	0.0254	0.0187	0.0136	0.0109
Proportion of Variance	0.7003	0.1647	0.0670	0.0363	0.0193	0.0124
Cumulative proportion	0.7003	0.8650	0.9320	0.9683	0.9876	1.0000
Eigenvector coefficients						
Humerus	-0.895	0.197	0.318	-0.018	0.236	0.061
Ulna	-0.894	0.286	-0.270	0.058	-0.198	-0.065
Metacarpal III	-0.849	0.369	0.377	0.023	0.017	0.014
Femur	-0.809	-0.403	0.024	-0.400	-0.098	0.116
Tibia	-0.800	-0.523	0.080	-0.064	0.101	-0.259
Metatarsal III	-0.722	-0.608	0.037	0.311	-0.030	0.100

Supplementary Table 3. Results of permanova statistic test of Mesozoic theropods in phylomorphospace of limb elements. The phylogeny backbone derived from the "mbl"-scaled super tree I. (*two-sided *p*-value threshold <0.05)

pairwise comparison	*F* Model	R^2	*p* (adjusted)
All limbs			
Avialae: non-avialan Paraves	11.969	0.146	0.003*
Avialae: non-paravian theropod	22.833	0.202	0.003*
non-avialan Paraves: non-paravian theropod	4.719	0.083	0.003*
Forelimb			
Avialae: non-avialan Paraves	2.653	0.037	0.171
Avialae: non-paravian theropod	19.609	0.179	0.003*
non-avialan Paraves: non-paravian theropod	4.540	0.080	0.003*
Hindlimb			
Avialae: non-avialan Paraves	23.564	0.252	0.003*
Avialae: non-paravian theropod	36.798	0.290	0.003*
non-avialan Paraves: non-paravian theropod	1.628	0.030	0.066

Supplementary Table 4. Results of conventional principal components analysis using the all limb, forelimb, and hindlimb of Mesozoic theropods.

	PC1	PC2	PC3	PC4	PC5	PC6
All limb						
Proportion of Variance	0.9394	0.0489	0.0063	0.0032	0.0011	0.0009
Eigenvector coefficients						
Humerus	0.363	0.325	-0.517	0.081	-0.496	-0.493
Ulna	0.292	0.533	-0.339	0.235	0.447	0.510
Metacarpal III	0.298	0.565	0.734	-0.166	-0.056	-0.148
Femur	0.508	-0.266	-0.155	-0.678	0.403	-0.156
Tibia	0.468	-0.286	0.102	-0.036	-0.563	0.609
Metatarsal III	0.466	-0.371	0.212	0.670	0.267	-0.282
Forelimb only						
Eigenvector coefficients						
Proportion of Variance	0.969	0.024	0.007			
Humerus	0.632	-0.625	-0.458			
Ulna	0.542	-0.065	0.837			
Metacarpal III	0.554	0.777	-0.298			
Hindlimb only						
Proportion of Variance	0.993	0.005	0.002			
Eigenvector coefficients						
Femur	0.608	-0.684	-0.404			
Tibia	0.561	0.009	0.828			
Metatarsal III	0.5628	0.730	-0.389			

Supplementary Table 5. Results of phylogenetically principal components analysis of the forelimb and hindlimb of Mesozoic theropods, separately. The phylogeny backbone derived from the "mbl"-scaled super tree I.

	PC1	PC2	PC3
Forelimb			
Standard deviation	0.0707	0.0257	0.0136
Proportion of Variance	0.8553	0.1132	0.0315
Cumulative proportion	0.8553	0.9685	1.0000
Eigenvector coefficients			
Humerus	0.918	-0.314	0.240
Ulna	0.944	-0.245	-0.223
Metacarpal III	0.914	0.405	0.019
Hindlimb			
Standard deviation	0.0545	0.0210	0.0116
Proportion of Variance	0.8380	0.1243	0.0377
Cumulative proportion	0.8380	0.9623	1.0000
Eigenvector coefficients			
Femur	-0.886	0.445	0.129
Tibia	-0.952	0.008	-0.303
Metatarsal III	-0.913	-0.389	0.126

Supplementary Table 6. Results of Welch's t-test of Mesozoic theropods in disparity metrices of all limb elements. The phylogeny backbone derived from the "mbl"-scaled super tree I. (*two-sided *p*-value threshold <0.05)

pairwise comparison	t	df	*p*
Sum of variances			
Avialae: non-avialan Paraves	-44.16	1066.4	2.2e-16*
Avialae: non-paravian theropod	-144.32	1079.1	2.2e-16*
non-avialan Paraves: non-paravian theropod	-66.415	1983.3	2.2e-16*
Median distance from centroids			
Avialae: non-avialan Paraves	-32.889	1173.6	2.2e-16*
Avialae: non-paravian theropod	-120.45	1191.5	2.2e-16*
non-avialan Paraves: non-paravian theropod	-62.109	1993.1	2.2e-16*
Sum of ranges			
Avialae: non-avialan Paraves	-4.5494	1398.3	5.85e-06*
Avialae: non-paravian theropod	-143.46	1665.4	2.2e-16*
non-avialan Paraves: non-paravian theropod	-96.186	1839	2.2e-16*

Supplementary Table 7. Results of Welch's t-test of Mesozoic theropods in disparity metrices of forelimb elements. The phylogeny backbone derived from the "mbl"-scaled super tree I. (*two-sided *p*-value threshold <0.05)

pairwise comparison	t	df	*p*
Sum of variances			
Avialae: non-avialan Paraves	-53.878	1176.3	2.2e-16*
Avialae: non-paravian theropod	-136.14	1057.4	2.2e-16*
non-avialan Paraves: non-paravian theropod	-91.984	1589.2	2.2e-16*
Median distance from centroids			
Avialae: non-avialan Paraves	-42.455	1181.7	2.2e-16*
Avialae: non-paravian theropod	-105.24	1142.4	2.2e-16*
non-avialan Paraves: non-paravian theropod	-52.228	1968.6	2.2e-16*
Sum of ranges			
Avialae: non-avialan Paraves	-22.294	1948.3	5.85e-06*
Avialae: non-paravian theropod	-171.9	1650.5	2.2e-16*
non-avialan Paraves: non-paravian theropod	-146.65	1809.5	2.2e-16*

Supplementary Table 8. Results of Welch's t-test of Mesozoic theropods in disparity metrices of hindlimb elements. The phylogeny backbone derived from the "mbl"-scaled super tree I. (*two-sided *p*-value threshold <0.05)

pairwise comparison	t	df	*p*
Sum of variances			
Avialae: non-avialan Paraves	-31.124	1093.6	2.2e-16*
Avialae: non-paravian theropod	-73.551	1259.9	2.2e-16*
non-avialan Paraves: non-paravian theropod	-12.818	1631.9	2.2e-16*
Median distance from centroids			
Avialae: non-avialan Paraves	-21.109	1395.6	2.2e-16*
Avialae: non-paravian theropod	-44.385	1687.5	2.2e-16*
non-avialan Paraves: non-paravian theropod	-11.853	1815.1	2.2e-16*
Sum of ranges			
Avialae: non-avialan Paraves	5.9162	1384.2	4.147e-09*
Avialae: non-paravian theropod	-53.515	1860.5	2.2e-16*
non-avialan Paraves: non-paravian theropod	-39.758	1622.3	2.2e-16*

Supplementary Table 9. Results of permanova statistic test of Mesozoic theropods in morphospace of limb elements from conventional PCA. (*two-sided *p*-value threshold <0.05)

pairwise comparison	*F* Model	R^2	*p* (adjusted)
All limbs			
Avialae: non-avialan Paraves	13.307	0.160	0.003*
Avialae: non-paravian theropod	25.289	0.217	0.003*
non-avialan Paraves: non-paravian theropod	6.600	0.114	0.003*
Forelimb			
Avialae: non-avialan Paraves	7.236	0.094	0.009*
Avialae: non-paravian theropod	33.591	0.270	0.003*
non-avialan Paraves: non-paravian theropod	5.597	0.099	0.018*
Hindlimb			
Avialae: non-avialan Paraves	22.328	0.242	0.003*
Avialae: non-paravian theropod	59.506	0.395	0.003*
non-avialan Paraves: non-paravian theropod	10.291	0.168	0.003*

Supplementary Table 10. Results of Welch's t-test of Mesozoic theropods in brachial index (BI) and crural index (CI). For comparison, CI_1 was calculated as differently for avialan and non-avialan theropods; CI_2 was calculated as the length ratio between tibiotarsus and femur for all taxa (see Methods for detail). The phylogeny backbone derived from the "mbl"-scaled super tree I. (*two-sided *p*-value threshold <0.05)

pairwise comparison	t	df	*p*
BI			
Avialae: non-avialan Paraves	-28.47	1284.6	2.2e-16*
Avialae: non-paravian theropod	-95.421	1418.1	2.2e-16*
non-avialan Paraves: non-paravian theropod	-42.941	1919.6	2.2e-16*
CI_1			
Avialae: non-avialan Paraves	-58.953	1551.8	2.2e-16*
Avialae: non-paravian theropod	-14.946	1354.8	2.2e-16*
non-avialan Paraves: non-paravian theropod	56.773	1109.7	2.2e-16*
CI_2			
Avialae: non-avialan Paraves	35.415	1986.7	2.2e-16*
Avialae: non-paravian theropod	79.337	1381.1	2.2e-16*
non-avialan Paraves: non-paravian theropod	37.483	1437.5,	2.2e-16*

Supplementary Table 11. Effective sample size of two independent runs for all limbs, forelimb, hindlimb, brachial index (BI), and crural index (CI), respectively, using the Gelman and Rubin's convergence diagnostic.

		Lh	Lh Prior	No. Pram	Alpha	Sigma.2
All limb	Chain 1	1517.6504	1205.1763	6428.4940	7617.2571	148.4034
	Chain 2	1460.5074	2128.3959	10135.5387	9704.0152	318.1652
Forelimb	Chain 1	3925.7345	2662.1496	9180.1502	35612.9061	314.6418
	Chain 2	1851.4398	1208.0387	8977.7930	49586.7965	117.1335
Hindlimb	Chain 1	1429.9538	691.3173	7815.7435	4988.8258	100.0593
	Chain 2	2031.6816	1512.8994	10415.5941	4484.4215	259.6385
BI	Chain 1	7784.9700	14199.3544	11439.3808	30112.7097	343.1401
	Chain 2	8317.9105	13531.0866	8753.8852	26273.4636	810.0119
CI	Chain 1	5375.4899	14659.3422	9146.8541	36672.2498	420.8991
	Chain 2	5454.1912	14211.4586	11691.2240	36354.6807	353.8873